

1 Radiation belt electron precipitation by manmade VLF transmissions

2 Rory J. Gamble and Craig J. Rodger

3 Department of Physics, University of Otago, Dunedin, New Zealand

4 Mark A. Clilverd

5 Physical Sciences Division, British Antarctic Survey (NERC), Cambridge, United Kingdom

6 Jean-André Sauvaud

7 Centre d'Étude Spatiale des Rayonnements, Toulouse, France

8 Neil R. Thomson, S. L. Stewart, and Robert J. McCormick

9 Department of Physics, University of Otago, Dunedin, New Zealand

10 Michel Parrot

11 Laboratoire de Physique et Chimie de l'Environnement, Orleans, France

12 Jean-Jacques Berthelier

13 Centre d'Études des Environnements Terrestre et Planétaires, Saint Maur des Fosses, France

14

15 **Abstract.** Enhancements of drift-loss cone fluxes in the inner radiation belt have been
16 observed to coincide with the geographic location of the powerful VLF transmitter NWC. In
17 this paper we expand upon the earlier study to examine the occurrence frequency of drift-loss
18 cone enhancements observed above transmitters, the intensity of the flux enhancements, and to
19 demonstrate the linkage to transmitter operation. Our study has confirmed the strong
20 dependence that these enhancements have upon nighttime ionospheric conditions. No
21 enhancements were observed during daytime periods, consistent with the increased ionospheric

22 absorption. We have also confirmed the persistent occurrence of the wisp features east of the
23 NWC transmitter. The enhancements are initially observed within a few degrees west of NWC,
24 and are present in 95% of the nighttime orbital data east of the transmitter for time periods
25 when the transmitter is broadcasting. No enhancements are observed when NWC is not
26 broadcasting. This provides conclusive evidence of the linkage between these drift-loss cone
27 electron flux enhancements and transmissions from NWC. When contrasted with periods when
28 NWC is non-operational, there are typically ~ 430 times more 100-260 keV resonant electrons
29 present in the drift-loss cone across $L=1.67-1.9$ due to NWC transmissions. There are almost no
30 wisp-like enhancements produced by the transmitter NPM, despite its low-latitude location and
31 relatively high output power. The lack of any wisp enhancement for $L < 1.6$ suggests that non-
32 ducted propagation is an inefficient mechanism for scattering electrons, which explains the
33 lower cutoff in L of the NWC-generated wisps and the lack of NPM-generated wisps.

34 **1. Introduction**

35 The behavior of high energy electrons trapped in the Earth's Van Allen radiation belts has been
36 extensively studied, through both experimental and theoretical techniques. During quiet times,
37 energetic radiation belt electrons are distributed into two belts divided by the "electron slot" at
38 $L \sim 2.5$, near which there is relatively low energetic electron flux. In the more than four decades
39 since the discovery of the belts [*Van Allen et al.*, 1958; *Van Allen*, 1997], it has proven difficult
40 to confirm the principal source and loss mechanisms that control radiation belt particles [*Walt*,
41 1996]. It is well known that large scale injections of energetic particles into the outer radiation
42 belts are associated with geomagnetic storms which can result in a 10^5 -fold increase in the total
43 trapped electron population [*Li and Temerin*, 2001]. In some cases the relativistic electron fluxes
44 present in the radiation belts may increase by more than two orders of magnitude [*Reeves et al.*,

45 2003]. In most cases, however, these injections do not penetrate into the inner radiation belt.
46 Only in the biggest storms, for example November 2003, does the slot region fill and the inner
47 belt gain a new population of energetic electrons [e.g., *Baker et al.*, 2004].

48 Even before the discovery of the radiation belts, high altitude nuclear explosions (HANEs) were
49 studied as a source for injecting electrons in the geomagnetic field. This was confirmed by the
50 satellite Explorer IV in 1958, when three nuclear explosions conducted under Operation Argus
51 took place in the South Atlantic, producing belts of trapped electrons from the β -decay of the
52 fission fragments. The trapped particles remained stable for several weeks near $L=2$, and did not
53 drift in L or broaden appreciably [*Hess*, 1968]. Following on from Operation Argus, both the US
54 and USSR conducted a small number of HANEs, all of which produced artificial belts of trapped
55 energetic electrons in the Earth's radiation belts. One of the most studied was the US "Starfish
56 Prime" HANE, a 1.4 Megaton detonation occurring at 400 km above Johnston Island in the
57 central Pacific Ocean on 9 July 1962. Again an artificial belt of trapped energetic electrons was
58 injected, although over a wide range of L -shells from about $L=1.25$ out to perhaps $L=3$ [*Hess*,
59 1968]. The detonation also caused artificial aurora observed as far away as New Zealand, and an
60 electromagnetic pulse which shut down communications and electrical supply in Hawaii,
61 1300 km away [*Dupont*, 2004].

62 The artificial belts produced by this Starfish Prime HANE allowed some understanding of the
63 loss of energetic electrons from the radiation belts, as demonstrated by the comparison of
64 calculated decay rates with the observed loss of injected electrons (Figure 7.3 of *Walt* [1994]).
65 Collisions with atmospheric constituents are the dominant loss process for energetic electrons
66 (>100 keV) only in the inner-most parts of the radiation belts ($L<1.3$) [*Walt*, 1996]. For higher L -
67 shells, radiation belt particle lifetimes are typically many orders of magnitude shorter than those
68 predicted due to atmospheric collisions alone, such that other loss processes are clearly

69 dominant. For example, one important loss process is driven by whistler mode waves, including
70 plasmaspheric hiss, lightning-generated whistlers, and manmade transmissions [*Abel and*
71 *Thorne, 1998, 1999; Rodger et al., 2003*].

72 It has been recognized that HANEs would shorten the operational lifetime of Low Earth
73 Orbiting satellites [*U.S. Congress, 2001; Steer, 2002*], principally due to the population of
74 HANE-injected >1 MeV trapped electrons. It has been suggested that even a "small" HANE
75 (~ 10 - 20 kilotons) occurring at altitudes of 125-300 km would raise peak radiation fluxes in the
76 inner radiation belt by 3-4 orders of magnitude, and lead to the loss of 90% of all low-earth-orbit
77 satellites within a month [*Dupont, 2004*]. In the event of a HANE, or an unusually intense
78 natural injection, this large population of valuable satellites would be threatened. Due to the
79 lifetime of the injected electrons, the manned space programme would need to be placed on hold
80 for a year or more. However, recent theoretical calculations have led to the rather surprising
81 conclusion that wave-particle interactions caused by manmade very low frequency (VLF)
82 transmissions may dominate non-storm time losses in the inner radiation belts [*Abel and Thorne,*
83 *1998; 1999*]. This finding has sparked considerable interest, suggesting practical human control
84 of the radiation belts [*Inan et al., 2003*] to protect Earth-orbiting systems from natural and
85 manmade injections of high energy electrons [*Rodger et al., 2006*]. This manmade control of the
86 Van Allen belts has been termed "Radiation Belt Remediation" (RBR).

87 Satellite observations of quasi-trapped ~ 100 keV electrons in the drift-loss cone have reported
88 "spikes" or enhancements in the flux population associated with the geomagnetic locations of
89 VLF transmitters [see *Datlowe and Imhof, 1990; and Datlowe, 2006; and references therein*].
90 Enhancements of drift-loss cone electron fluxes are expected eastwards of the transmitter
91 location, with cyclotron resonance taking place on field lines near the ground based VLF
92 transmitter, followed by the eastward drift of electrons towards the South Atlantic Anomaly.

93 Transmitters located under a nighttime ionosphere are likely to be more effective, due to the
94 lower ionospheric absorption of the upgoing transmitter waves. Proposed RBR systems have not
95 focused upon ground-based VLF transmitters, but they can serve as a test-bed for examining the
96 effectiveness of man-made control systems, and increasing our understanding of the wave-
97 particle interactions which are likely to underpin an operational RBR system.

98 Very recently, observations by the DEMETER microsatellite near the powerful VLF
99 transmitter NWC have shown that this transmitter causes electron and ion heating in the
100 ionosphere at 700 km, affecting a $\sim 500,000 \text{ km}^2$ region [Parrot *et al.*, 2007]. These authors also
101 presented DEMETER-measured increases in energetic electrons in the range 91-527 keV,
102 attributed to NWC. Following on from this study, a further examination of DEMETER wave
103 and particle data considered the significance of NWC upon electrons in the inner radiation belt,
104 showing that enhancements in the ~ 100 -600 keV drift-loss cone electron fluxes at low L values
105 are linked to NWC operation and to ionospheric absorption [Sauvaud *et al.*, 2008]. The
106 enhancements, termed 'wisps', are only detected eastward of the transmitter location, as
107 expected from the electron drift motion, and at energies that are consistent with first order
108 equatorial cyclotron resonance between the NWC transmissions and electrons interacting in the
109 vicinity of the magnetic equatorial plane. These authors conclude that the NWC transmitter is
110 extremely well positioned to have a potential influence upon inner radiation belt >100 keV
111 electrons.

112 Some previous authors have argued that non-ducted propagation will play an important role in
113 electron precipitation driven by ground-based VLF transmitters [Inan *et al.*, 2007], as non field-
114 aligned propagation allows high-order resonances hence driving the loss of higher energy
115 particles. It is generally accepted that there is no significant ducting below $L=1.6$ as the
116 plasmaspheric electron density increases which cause ducting are not sufficient below this

117 point. Recently, *Clilverd et al.* [2008] concluded that the transmissions from a VLF transmitter
118 located in Hawaii were wholly non-ducted as they propagated through the inner plasmasphere.
119 However, the same study found that the conjugate wave power from NWC stretched from
120 $L=1.4$ to $L=2.2$, arguing that the dominant propagation mechanism for $L=1.4$ to $L=1.6$ is non-
121 ducted, while ducted propagation dominates for $L>1.6$.

122 In this paper we expand upon the earlier *Sauvaud et al.* [2008] letter to provide additional
123 details as to the effect of transmissions from NWC on inner radiation belt electrons.
124 Specifically we examine the occurrence frequency of drift loss cone enhancements observed
125 above transmitters, the intensity of the flux enhancements, and clearly demonstrate the linkage
126 to transmitter operation. In addition, we consider the relative effectiveness of ducted and non-
127 ducted propagation on pitch angle scattering of inner radiation belt electrons.

128 **2. Instrumentation**

129 DEMETER is the first of the Myriade series of microsatellites, and was placed in a circular
130 Sun-synchronous polar orbit at an altitude of 710 km at the end of June 2004. Data are
131 available at invariant latitudes $<65^\circ$, providing observations around two local times ($\sim 10:30$ LT
132 and $22:30$ LT). The IDP particle instrument carried onboard DEMETER looks perpendicularly
133 to the orbital plane of the satellite, and thus detects fluxes of $\sim 90^\circ$ pitch angle electrons inside,
134 or just outside, the drift loss cone. This instrument is unusual in that it has very high energy
135 resolution; in normal "survey" mode the instrument measures electron fluxes with energies
136 from 70 keV to 2.34 MeV, using 128 energy channels every 4 seconds [*Sauvaud et al.*, 2006].
137 Energy resolution depends on the operational mode of the satellite, being either 17.8 keV in
138 "survey" mode or 8.9 keV in "burst" mode. All burst mode data we consider in our study were
139 downsampled to survey mode resolution in this study for homogeneity. The same spacecraft

140 also carries the ICE instrument, which provides continuous measurements of the power
141 spectrum of one electric field component in the VLF band [Berthelier *et al.*, 2006]. Here we
142 make use of both survey and burst mode data of the electric field spectra recorded up to
143 20 kHz, with a frequency channel resolution of 19.25 Hz.

144 In addition, we also make use of narrow-band subionospheric VLF data received at Dunedin,
145 New Zealand (45.9°S, 170.5°E) by an OmniPAL receiver, part of the Antarctic-Arctic
146 Radiation-belt Dynamic Deposition VLF Atmospheric Research Konsortia (AARDDVARK).
147 More information on AARDDVARK can be found at the website:
148 http://www.physics.otago.ac.nz/space/AARDDVARK_homepage.htm.

149 The powerful US Navy transmitter with call sign "NWC" (19.8 kHz, 1 MW radiated power,
150 North West Cape, Australia, $L=1.45$) is extremely well positioned to have a potential influence
151 upon >100 keV electrons in the inner radiation belt; most other powerful VLF transmitters are
152 located at much higher L -shells, leading to resonances with <10 keV electrons. The lefthand
153 panel of Figure 1 shows the average spectral power received by DEMETER's ICE instrument in
154 a ~195 Hz band centered on 19.8 kHz, for nighttime orbits occurring from 12 August - 26
155 September 2005. Throughout our study, DEMETER satellite locations are specified in
156 geographic coordinates which have been traced down the magnetic field line to an altitude of
157 100 km using the IGRF-2000 model, epoch 2005. The figure suppresses data coverage near the
158 geomagnetic equator as the results of the field tracing becoming incorrect at very low latitudes.
159 The location of NWC is shown by a green diamond, and the subionospheric great circle path
160 from NWC to Dunedin is also marked. In the DEMETER data, NWC produces high power
161 levels in both the source and conjugate hemispheres, although the conjugate location is shifted
162 polewards as discussed by *Cilverd et al.* [2008] due to non-ducted propagation through the
163 plasmasphere. The right-hand panel of Figure 1 shows the average spectral power received

164 from NWC for daytime orbits during the same time period. As can be seen in Figure 1
165 DEMETER also clearly observes NWC transmissions during the day in the same time period,
166 but at power levels which are typically ~ 1200 times (i.e. ~ 31 dB) lower due to increased
167 ionospheric absorption. This is reasonably consistent with the ~ 37 dB difference between the
168 estimated daytime and nighttime ionospheric absorption for a 20 kHz signal [*Helliwell*, Fig 3-
169 35, 1965]. For short-lived electromagnetic wave events, like whistlers, the pitch angle
170 scattering efficiency is proportional to whistler-mode wave field amplitude rather than power
171 [e.g. *Chang and Inan*, 1983]. However, in the case of a long-lasting electromagnetic wave field
172 produced from a continuously operating VLF transmitter, particles bounce (and interact with
173 the waves) many times while crossing the illuminated region, and while each individual pitch
174 angle change is proportional to field amplitude, there is a random phase so the cumulative
175 effect is roughly diffusive. In this case the scattering "efficiency" should scale linearly with
176 power, suggesting that the transmissions from NWC should be ~ 1200 times more effective at
177 scattering energetic electrons towards the loss cone during local nighttime.

178 Subionospheric signals from NWC received at Dunedin are >40 dB above the noise floor,
179 allowing us to use these observations to confirm NWC on and off periods. Figure 2 shows the
180 UT typical variation in NWC transmissions received in Dunedin, in this case shown in the form
181 of 1-minute average amplitudes measured from 21-28 August 2005. The typical diurnal
182 amplitude variation spans 15-16 dB, with smoothly varying amplitudes during the period where
183 the lower edge of the ionosphere is illuminated by the Sun, and higher amplitudes during the
184 night. During the daytime period of 22 August the transmitter did not broadcast for ~ 7 hours,
185 and the amplitude drops by ~ 50 dB down to the noise floor. This is the weekly maintenance
186 period for this transmitter and reflects the pattern of operation of US Navy transmitters during
187 normal operations, i.e., near-constant broadcasting (roughly 95% of the time).

188 3. Drift-loss cone observations

189 Particle measurements by the IDP instrument were examined for DEMETER orbits in the
190 time period 12 August-26 September 2005 when the spacecraft passed within $\pm 25^\circ$ longitude of
191 NWC's location. While our time period included significant geomagnetic storms [e.g., *Rodger*
192 *et al.*, 2007a] IDP-observations indicate that these storms did not produce significant radiation
193 belt electron flux enhancements at $L < 2$. For clarity, only observations taken when DEMETER
194 was located in NWC's hemisphere (i.e., the southern hemisphere) were considered. Under these
195 constraints there were 173 half-orbits examined, of which 84 were for nighttime conditions,
196 that is, when the ionosphere is not illuminated by the Sun. A significant number of the orbits
197 contain enhancements of drift-loss cone electron fluxes with a characteristic pattern; throughout
198 this study we will term such enhancements "wisps", following *Sauvaud et al.* [2008]. A set of
199 four typical wisps are shown in Figure 3, presenting the IDP instrument-measured differential
200 electron fluxes in units of electrons $\text{cm}^{-2}\text{s}^{-1}\text{sr}^{-1}\text{keV}^{-1}$ during these events. The four panels
201 present wisps on 27 August 2005 (starting at 13:59 UT, 14.2 min long, 24° east of NWC), 3
202 September 2005 (13:15 UT, 13.9 min, 22° east), 4 September 2005 (13:59 UT, 14.0 min, 12°
203 east), and 20 September 2005 (\sim 3:59 UT, 14.1 min, 12° east). The wisp features are very clear
204 in these passes; for example, on 27 August 2005 the wisp is the feature which starts at $L \approx 1.6$
205 and ~ 350 keV, and decreases in energy with increasing L , as expected from cyclotron
206 resonance [e.g., *Chang and Inan*, 1983]. The enhanced electron flux seen in all panels for $L > 2$
207 is a consistent feature associated with the energy-structure of the radiation belts. Both the
208 features of our wisps and the energy structure in the inner radiation belt are essentially the same
209 as those shown in Figure 1 of *Datlowe* [2006], where the single "wisp" shown was attributed to
210 field-aligned, first order, cyclotron resonance with transmissions from NWC.

211 Table 1 summarizes our observations of wisps comparing occurrence rates to the west and
212 east of NWC, and also separated into nighttime and daytime orbits. The first value given in
213 each cell of the table is the number of half-orbits examined, while the second value gives the
214 number of those half-orbits which have been observed to contain wisps. Clearly, the vast
215 majority of wisps are observed in the orbits which are within 25° east of NWC. Additionally,
216 wisps are observed only during nighttime half-orbits, almost certainly due to the much lower
217 ionospheric absorption of NWC transmissions through the nighttime ionosphere. Of the three
218 eastern nighttime half orbits for which no wisp was observed, NWC was not transmitting for
219 one of these times, although was transmitting for the other two times. Thus for nighttime
220 conditions, DEMETER observations show that when broadcasting NWC creates "down stream"
221 drift-loss enhancements of >100 keV electrons ~95% of the time, but is unable to produce a
222 significant effect under a daytime ionosphere. These enhancements will drift around the Earth
223 to the South Atlantic Anomaly, where they will precipitate into the atmosphere. A small
224 number of wisps were observed during nighttime orbits occurring west of NWC (~22% of the
225 time), with all but one of these wisps occurring within 6° longitude of the transmitter. Although
226 less common this is consistent with an NWC-driven scattering mechanism, as the longitudinal
227 extent of the NWC transmissions is significant, as shown in Figure 1. VLF transmitters located
228 westward of NWC, for example in Europe are unlikely to be the source of those wisps observed
229 slightly to the west of NWC's location. European transmitters are located conjugate to the
230 eastern edge of the South Atlantic Anomaly, and hence any electrons under-going pitch angle
231 scattering from these transmitters are likely to be driven into the local bounce loss cone and lost
232 immediately into the conjugate atmosphere. In addition, Figure 2 of *Sauvaud et al.* [2008]
233 shows no significant enhancement in the 200 keV fluxes to the west of NWC's location, and an

234 enhancement which stretches from NWC's approximate location eastwards to the South
235 Atlantic Anomaly.

236 **4. Wisp Event Link to NWC operation**

237 During the 12 August-26 September 2005 study period selected, NWC generally operated in
238 its normal mode of near-continuous broadcast punctuated by regular ~7 hour maintenance
239 periods (Figure 2). In general, it is very rare for NWC to be non-operational during local
240 nighttime. However, subionospheric measurements of NWC received at Dunedin show that
241 NWC was not transmitting throughout the period from ~22:00 UT on 13 June 2005 through to
242 06:18 UT on 28 June 2005 (Figure 4). Over this time period, there were 8 nighttime DEMETER
243 half-orbits within 25° longitude eastwards of NWC. None of these orbits showed wisps in the
244 drift-loss cone fluxes. The circles marked in Figure 4 indicate the times of DEMETER
245 nighttime orbits east of NWC, while crossed circles show orbits in which wisps were observed.
246 Wisps were seen immediately before, and after, the NWC off time period, when NWC was
247 transmitting normally. These observations provide conclusive evidence of the linkage between
248 wisps and transmissions from NWC.

249 As an additional test, we examine the long term observations of inner radiation belt electrons
250 in 2007. From 1 July 2007 through to about 22 January 2008, NWC did not transmit. Figure 5
251 shows a world map of the combined >100 keV electron counts from the 90° electron telescopes
252 on the NOAA-15,-16,-17, and -18 POES spacecraft for the time period 1 August to 31
253 December 2007. The latitude and longitude shown is the geographic position of the sub-
254 satellite point. In order to increase the sensitivity of our test, we combine all the 16 s electron
255 integral flux observations provided by NOAA's National Geophysical Data Center, by
256 summing the observations for all times in that period from all the satellites, with 1 degree

257 resolution. The 90° electron telescope of the Medium Energy Proton and Electron Detector
258 (MEPED) instrument detects trapped and quasi-trapped electrons in the inner radiation belt.
259 This can be seen from the top panel of Figure 4, where the inner belt fluxes increase
260 considerably from ~75°E eastwards to ~250°E. This panel shows the expected structure of the
261 radiation belts, with the inner and outer belts separated by the slot region, and the South
262 Atlantic Magnetic Anomaly. NWC operated normally in the first part of 2007. The lower panel
263 of Figure 5 shows the ratio between the period 1 Jan-31 May 2007, when NWC was
264 broadcasting normally and the period 1 Jul- 31 Dec 2007 (upper panel) when NWC was off.
265 The POES-observed >100 keV electron fluxes increase by ~5-7 times from the longitude of
266 NWC through to the South Atlantic Magnetic Anomaly, due to the operation of NWC. This
267 difference is more significant than the variation in slot region fluxes, likely to be due to
268 seasonal variations in plasmaspheric hiss occurrence and plasmaspheric densities.

269 We have also examined the MEPED >100 keV 0° electron telescope observations. At NWC-
270 latitudes this should be measuring electrons in the bounce loss cone. However, we do not see
271 any indication of enhanced bounce loss cone fluxes around NWC. This is likely to be due to the
272 sensitivity of the instrument, as the expected distribution of whistler-generated electron
273 precipitation [Rodger *et al.*, 2007b] is also not present in this data, which is likely to be more
274 intense in some regions than the NWC-driven losses into the bounce loss cone.

275 **5. Relative electron flux enhancements in wisp events**

276 In order to examine the magnitude of wisp events they are compared to the electron flux
277 observed by DEMETER across the same L-shell range on 29 August 2005 from 14:36-
278 14:49 UT. NWC was not transmitting in this time period, and this is one of the 3 nighttime
279 orbits east of NWC for which no wisp was present. We use these fluxes to provide an

280 indication of the undisturbed electron drift-loss electron fluxes, and thus to determine the
281 significance of NWC-driven scattering. An example of this is shown in Figure 6, where the
282 relative flux enhancements are presented for the 4 wisp events shown in Figure 3. In the L -shell
283 range below $L=2$, there is generally agreement between the electron densities measured outside
284 the wisp features and the "non-disturbed" fluxes from 29 August 2005. Above $L=2$ there can be
285 differences of several orders of magnitude, due to variations in the fluxes in the electron slot
286 region. The 4 panels of Figure 6 are representative of wisp events observed. Typically, the wisp
287 flux values in a single event are approximately at a constant multiplicative value above the
288 background quasi-trapped electron fluxes in the drift-loss cone. This implies that the efficiency
289 of the pitch-angle scattering mechanism which produces wisps is linear in both energy and L -
290 range. Table 2 provides a summary of the typical L -shell, energy range, and enhancement
291 factor for the 46 wisps observed in the August-September 2005 period. Typically, the wisps
292 extend from $L=1.67$ - 1.9 , although the upper L -cutoff is likely to be limited by the lower energy
293 threshold for the IDP instrument. Wisp events can have a fairly varied upper energy, ranging
294 from ~ 120 - 410 keV, and also a wide range of enhancement factors, with the peak flux
295 enhancement ranging from ~ 1.2 times to 2200 times the reference spectrum with a (geometric)
296 mean enhancement factor of ~ 430 . Thus, there are typically ~ 430 times more 100-260 keV
297 resonant electrons present in the drift-loss due to NWC transmissions compared with periods
298 when NWC is non-operational.

299 After the 13-28 June 2005 NWC off time period, one might expect the wisp enhancements to
300 be larger, due to a buildup in fluxes during the off time. No such difference is observed in the
301 wisp flux levels once NWC resumes operation, although it is questionable if such an increase
302 would be detectable when compared with the large variation in wisp enhancements during
303 constant NWC operation. In addition, it should be noted that the first wisp observation after the

304 transmitter's non-operational period occurs at 13:27 UT on 29 Jun 2005, ~31 hours after the
305 transmitter resumes operation. Compared to the electron drift period of ~4-5 hours in this
306 energy and L shell range (once around the Earth), it is more likely than any increase in wisp
307 enhancements due to this effect will have been "flushed out" such that it is not discernable in
308 this dataset by the time the craft has the opportunity to measure it.

309 The significance of the NWC loss cone enhancements have been estimated through
310 comparison with the AE-5 Inner Zone Electron Model [*Teague and Vette, 1972*]. This model
311 provides analytic functions for the unidirectional differential energy flux and is based on data
312 collected during solar maximum conditions. The analytic functions in AE-5 describe quiet-day
313 electron fluxes for $1.3 \leq L \leq 2.4$ and are based on observations of electrons with $E < 690$ keV.
314 Transmissions from NWC typically scatter into the drift loss cone roughly 0.05% of the AE-5
315 described electrons with resonant energy (i.e., $E=168$ keV at $L=1.77$) in a magnetic flux tube
316 with 1 cm^2 square cross section at 100 km. In contrast, a 0.5-10 kHz whistler will typically
317 scatter 0.005% of the resonant electrons of a given energy into the bounce loss cone (following
318 the approach of *Rodger et al. [2003]*). However, we note that this is not a like with like
319 comparison, as the resonant energies for the whistler at $L=1.77$ span 330-2900 keV.

320 **6. Comparison with cyclotron resonance calculations**

321 Figure 7 shows the predicted variation with L of the first-order cyclotron resonant energy for
322 energetic electrons resonant at the geomagnetic equator with 19.8 kHz waves (black),
323 determined from the expressions in *Chang and Inan [1983]*. The resonant energy is strongly
324 dependent upon the plasmaspheric electron density, shown in Figure 7 by the gray dotted line.
325 The plasmaspheric electron densities used were interpolated using two sets of experimental
326 observations from $L=2.2$ and $L=1.4$. The higher L -shell measurements come from the ISEE 1

327 satellite and whistler based mid-solar cycle results of *Carpenter and Anderson* [1992]. The
328 lower L -shell measurements come from the Alouette-2 satellite results of *Mahajan and Brace*
329 [1969] near $L=1.4$ (altitudes ~ 2500 km) for the period May 1966-March 1967. In Figure 7 the
330 crosses show the median wisp values for L and energy from Table 2. Thus there is very good
331 agreement between the calculations and a typical wisp, providing additional evidence that the
332 wisps are generated by first-order cyclotron resonance with 19.8 kHz waves from NWC, with
333 the interaction taking place at or near the geomagnetic equator. The lowest energy of the NWC-
334 generated wisps is close to the lowest energy channel observed by the IDP instrument, so that
335 enhancements at higher L -shells will be below this energy floor. The lower L and upper energy
336 limits are likely to be due to the propagation mode of NWC through the plasmasphere, as
337 discussed in the following section. A similar high-quality fit between resonant energy
338 calculations and a wisp event [*Sauvaud et al.*, Fig. 3, 2008] was determined using a totally
339 different plasmaspheric electron density model, indicating the robustness of these calculations.

340 **7. Comparison with other VLF transmitters**

341 Clearly NWC produces a very strong feature in the quasi-trapped electron fluxes for energies
342 of a few hundred keV and in the L -shell range of ~ 1.67 to ~ 1.9 , which is well predicted by first-
343 order cyclotron resonance. It is interesting to consider whether DEMETER can observe drift-
344 loss cone enhancements produced by other VLF transmitters. As noted above, VLF transmitters
345 in Europe lie in the conjugate region to the eastern edge of the South Atlantic Anomaly, and
346 hence will not lead to an enhancement in drift-loss cone electrons, as any electrons will be
347 driven into the local bounce cone and lost immediately into the conjugate atmosphere. Should
348 this be taking place, it would be challenging to detect in DEMETER observations. Similarly,
349 the powerful US Navy transmitter, NAA, on the east coast of the United States is conjugate to

350 the western edge of the South Atlantic Anomaly. Assuming that the resonant energies will also
351 be governed by first-order resonance, the L -shells of NAA and the majority of the European
352 transmitters suggest their transmissions will be resonant with relatively low energy electrons
353 (<100 keV), often below the lower-cutoff for DEMETER IDP observations.

354 One other possible transmitter candidate for producing significant detectable drift-loss
355 enhancements (in addition to NWC) is the ~ 500 kW US Navy communications station with
356 call-sign NPM broadcasting at 21.4 kHz from Hawaii ($L=1.17$). Observations from the
357 DEMETER spacecraft in the hemisphere conjugate to NPM indicate the transmitted power
358 spreads across $L=1.2$ to $L=1.5$ [Clilverd *et al.*, 2008]. If the NPM transmissions interacted with
359 inner radiation belt electrons through first-order resonance, the resonant energies would be
360 high, for example 700 keV at $L=1.4$ and 450 keV at $L=1.5$. We examined DEMETER orbits
361 from 12 August - 26 September 2005 which passed within 25° longitude east of NPM in the
362 northern hemisphere. During this time NPM was largely broadcasting in the standard US Navy
363 pattern of operation, and hence was operational near-continuously. The majority of the 37 NPM
364 orbits occurring in daylight contained wisps occurring over the same L -shell and energy range
365 as previously observed to be produced by NWC. At these times there was a nighttime
366 ionosphere above NWC, and hence NWC wisp generation is expected, as NWC-generated
367 wisps will drift to NPM's longitude in ~ 70 minutes or less, depending on energy. Conversely,
368 when there was a nighttime ionosphere above NPM, NWC would be day lit, which removes the
369 possibility of NWC-generated wisps. We examined 36 orbits eastwards of nighttime NPM.
370 Thirty-five of them showed no detectable enhancement in the quasi-trapped electron fluxes
371 (i.e., no wisps). The left panel of Figure 8 shows a typical orbit from this period on 19 August
372 2005, starting at $\sim 07:34$ UT. Even though NPM radiates roughly half the output power of NWC
373 and thus might be expected to produce an enhancement at least 200 times the background, no

374 wisp-features are present in this case. In the L -region from 1.2 to 1.5 where wisps might be
375 expected due to non-ducted NPM transmissions, the quasi-trapped electron fluxes are ~ 10
376 times higher than for the orbits east of NWC shown in Figure 3, due to the steady filling of the
377 drift loss cone with eastward drift. Nonetheless, the NWC-generated wisps are still clear in the
378 NPM daytime orbit data, and thus we would expect evidence for non-ducted NPM-generated
379 wisps despite the higher background levels. Only one of the nighttime orbits east of NPM
380 contains a wisp, occurring across the L -range 1.6 to 1.725 as shown in the right panel of Figure
381 8. This single wisp event is consistent with ducted NPM propagation leading to an
382 enhancement around 190 keV at $L=1.7$, as outlined below.

383 As noted above, transmitters at $L < 1.6$ will propagate through the plasmasphere in a non-
384 ducted manner, while those beyond appear to be largely ducted [*Cilverd et al.*, 2007]. This
385 study indicated that NPM transmissions were largely non-ducted, and argued that the
386 transmissions from NWC would be non-ducted from $L=1.4$ to $L=1.6$ and ducted up to $L=2.2$
387 (the highest L -shell for which conjugate transmissions from NWC were observed). The
388 resonance energies for NWC-generated wisps are consistent with solely first-order field-aligned
389 resonance starting at $L=1.6$, i.e., consistent with ducted propagation starting at this L -shell.
390 Non-ducted propagation leads to significantly higher resonance energies than first-order
391 resonances for field aligned propagation. *Datlowe and Imhoff* [1990] found the resonance
392 energy almost doubled as the angle changed from 0° (field aligned) to 70° . The lack of any wisp
393 enhancement for $L < 1.6$ suggests that non-ducted propagation is an inefficient mechanism for
394 scattering electrons, which explains the lower cutoff in L of the NWC-generated wisps and the
395 lack of NPM-generated wisps. Calculations of >100 keV electron precipitation from ground-
396 based transmitters based on non-ducted propagation through the magnetosphere predicts that
397 the >100 keV flux due to NWC at $L=1.7$ should be only 25% higher than that due to

398 transmissions from NPM [Kulkarni *et al.*, 2008]. This study also suggests that the peak in
399 NWC-driven scattering of >100 keV electrons should lie at about $L=2$, which is outside the
400 range of the wisp events observed in DEMETER, and inconsistent with the observations
401 reported in the current study. In practice it is not clear in the DEMETER data that there is any
402 non-ducted electron scattering from either transmitter, with the single NPM scattering event
403 observed consistent with a ducted wave, despite the small differences expected from non-
404 ducted calculations.

405 While Figure 1 shows there is somewhat less power from NWC observed at DEMETER in the
406 $L=1.4-1.6$ conjugate region when contrasted with $L=1.6-1.8$, our observed wisps start suddenly
407 at $L\approx 1.6$ (where ducting starts). This implies that NWC is one of the few transmitters for which
408 there will be regular scattering of >100 keV electrons which can be easily detected by satellites
409 as they drift around the Earth. The Italian VLF transmitter (40.9°N , 9.8°E , $L=1.45$) should
410 produce significant ducted signals, but due to its location near the anomaly these transmissions
411 will scatter electrons directly into the local bounce loss cone. In contrast, the Indian transmitter
412 (8.45°N , 77.75°E , very near the magnetic equator) and Japanese transmitter (32°N , 130.8°E ,
413 $L=1.23$) will be much like NPM, rarely coupling into ducts and thus not producing significant
414 scattering due to their non-ducted propagation through the plasmasphere. The majority of the
415 remaining VLF transmitters are at higher L , and hence the transmissions from these transmitters
416 will resonant with lower-energy electrons.

417 If the NWC-generated wisps are produced solely by ducted propagation of NWC through the
418 plasmasphere, it is reasonable to question if ducts are large enough to span from $L=1.6$ to at
419 least $L=1.91$, and also whether ducts might be expected to be present at longitudes very close to
420 NWC $\sim 95\%$ of the time. An effective method of testing this idea is to use data from a ground-
421 based experiment that monitors the signals produced by a large VLF transmitter similar to

422 NWC that have propagated through the plasmasphere as ducted whistler-mode waves. Well
423 located, near-conjugate, observations of whistler mode signals from the powerful US Navy
424 VLF transmitter in Cutler, Maine (NAA, 24.0 kHz) have been made in Antarctica almost
425 continuously since 1986 [*Clilverd et al.*, 1991; 2000]. For more than two solar cycles close to
426 100 percent of nights have shown one hop whistler mode signals when the transmitter has been
427 on. Recordings have been made such that multi-hop whistler modes could be observed,
428 although to date none have been detected. This suggests that multi-hop whistler mode signals
429 from VLF naval transmitters are very rare, which is consistent with the lack of wave
430 amplification of NAA whistler mode signals reported by *Clilverd and Horne* (1996). Hence we
431 conclude that the DEMETER-observed wisps are likely due to the interaction with primarily
432 one-hop whistler mode transmitter signals.

433 Figure 9 shows a typical example of night time whistler-mode signals received at Rothera
434 station, Antarctica, (67.5°S , 68.1°W , $L=2.7$) due to transmissions from NAA. This transmitter
435 has a very similar output power to NWC. The plot shows the amplitude of received NAA
436 whistler-mode signals arriving at Rothera as a function of group delay time. The group delays
437 are indicative of night time ducted propagation between $L=1.6$ and $L=2.6$ as indicated by two
438 horizontal dashed lines. Also shown on the plot are subionospheric mountain reflections, which
439 have very low delay compared with the arrival time of the direct, subionospheric signal
440 [*Thomson*, 1989], and software calibration signals of known amplitude. A similar plot for NPM
441 has been presented by [*Thomson*, Fig. 4, 1987].

442 The lower L -shell limit of the whistler mode signals at $L=1.6$ in Figure 9 is consistent with the
443 ducted whistler-mode propagation seen in the previous figures of the current study, and the
444 upper limit at $L=2.6$ is consistent with the half-gyrofrequency cutoff for inter-hemispheric
445 ducted propagation [*Clilverd et al.*, 2008]. From the data in Figure 9 we can see that although

446 individual ducts are present across many L -shells (group delays), there is a general spread of
447 whistler mode power in the range $1.6 < L < 2.6$, and of particular interest here, across $L=1.67-1.9$,
448 which can explain the uniform L -shell spread of NWC-generated wisp flux enhancements
449 observed by DEMETER. Long-term studies of NAA from the Antarctic Peninsula have also
450 shown that ducts are observed at longitudes close to the transmitter almost every night of the
451 year [Clilverd *et al.*, 1993], which would be consistent with the 95% NWC wisp occurrence
452 rate observed. It seems possible that the ionospheric heating produced by the VLF transmitter,
453 as has been reported over NWC [Parrot *et al.*, 2007], may itself lead to the production of ducts
454 above the transmitter. This deserves further modeling.

455 **8. Discussion**

456 The US Air Force is to launch the Demonstrations and Science Experiment (DSX) mission in
457 2009, which will include the Radiation Belt Remediation experiment with a 50 m antenna to
458 "demonstrate the viability of VLF RBR techniques" [Winter *et al.*, 2004]. The VLF payload of
459 this mission is to include a transmitter to broadcast up to the kilowatt level in the range 1-
460 50 kHz. The power of the NWC transmissions received by DEMETER during the night at the
461 transmitter's latitude falls off as the longitudinal difference between the spacecraft and the
462 transmitter increases, as expected. When contrasted with the signal powers calculated by the
463 LWPC propagation model [Ferguson and Snyder, 1990] at the equivalent locations but below
464 the night time ionosphere, we find the DEMETER observations are approximately 1000-times
465 lower than those occurring below the ionosphere. In addition, the power of the DEMETER
466 received nighttime NWC-transmissions is observed to vary by about 2 orders of magnitude at
467 the same location but from orbit to orbit. This is likely to be the primary reason for the large
468 variations in the mean enhancement factor observed in wisps. Thus it appears that absorption

469 decreases the power of NWC transmissions during the nighttime by 10^2 - 10^4 times. As such
470 NWC is roughly equivalent to a ~ 0.1 - 10 kW space-based transmitter during night periods, and
471 a ~ 0.1 - 10 W transmitter during the day. Clearly, the transmissions from NWC provide an
472 additional and potentially useful route for testing RBR systems, while the RBR-instrument
473 onboard DSX is likely to produce smaller enhancements in the drift loss cone fluxes than those
474 due to the nighttime transmissions from NWC.

475 The mostly likely causes for the large variations in the wisp mean enhancement factor are
476 variations in the power of the NWC reaching the geomagnetic equator, or variations in the
477 inner radiation belt trapped electron population having pitch angles just above the loss cone.
478 Considering the first possibility, as mentioned above there is a very significant variation in the
479 power of NWC received at DEMETER during nighttime orbits, which should directly affect the
480 rate at which particles are scattered into the loss cone. There is not a direct relationship between
481 the DEMETER observed wisp enhancement and the DEMETER observed NWC power.
482 However, the locations where DEMETER observes a wisp is normally considerably eastwards
483 from the longitudes where the wave-particle interactions are taking place (i.e., very near to
484 NWC). As such the DEMETER observations are not well suited to test this. In contrast, the
485 DSX observations will be well suited for such a test. Considering the second possibility, the
486 IDP DEMETER instrument measures electrons in the drift loss cone, and as such is not well
487 suited for examining relationships between the wisp enhancement factor and trapped electron
488 flux levels. While one might argue that there should be a relationship between the fluxes just
489 inside and just outside the drift loss cone, we do not find any relationship between the wisp
490 enhancement factors and DEMETER observed non-wisp drift loss cone fluxes (i.e. for energies
491 just outside those of the wisp). In addition, it is likely that NWC will cause significant resonant
492 scattering at pitch angles far from the loss cone, which will contribute to the long term loss rate.

493 This will alter the pitch angle distribution of the trapped electrons, and deserves further study.
494 As another example of the effect of NWC on the inner radiation belts, we examined the
495 >100 keV quasi-trapped electron fluxes (those in and near the drift loss cone) observations
496 from the 4 POES spacecraft in the range $L=1.6-1.8$ varied by a factor of 20 during a 5 month
497 period in which NWC did not operate. The variation was considerably higher outside this time
498 period (peak variations of ~ 500 times). However, the August-September 2005 wisp
499 enhancements do not track with the POES observed variations, and it is not clear that these
500 parameters observed by the DEMETER and POES are linked.

501 **9. Summary and Conclusions**

502 Enhancements of drift-loss cone fluxes in the inner radiation belt have been observed to
503 coincide with the geographic locations of the powerful VLF transmitter NWC. *Sauvaud et al.*
504 [2008] demonstrated that enhancements in the $\sim 100-600$ keV drift-loss cone electron fluxes at
505 low L values are linked to NWC operation and to ionospheric absorption producing
506 enhancements, termed 'wisps', consistent with first order equatorial cyclotron resonance. While
507 proposed Radiation Belt Remediation systems have not focused upon ground-based VLF
508 transmitters, studies into how these transmitters interact with inner radiation belt electrons can
509 serve as a test-bed for examining the effectiveness of man-made control systems, and
510 increasing our understanding of the wave-particle interactions which are likely to underpin an
511 operational RBR system. *Sauvaud et al.* concluded that the NWC transmitter is extremely well
512 positioned to have a potential influence upon inner radiation belt >100 keV electrons. In this
513 paper we have expanded upon the earlier study by examining the occurrence frequency of drift
514 loss cone enhancements observed above transmitters, the intensity of the flux enhancements,
515 and by demonstrating the linkage to transmitter operation.

516 Our study has confirmed that these drift-loss-cone enhancements occur only at night. NWC
517 signals received at the satellite during the day are at power levels which are typically ~1200
518 times lower than at night due to the much higher ionospheric absorption, suggesting that
519 nighttime transmissions from NWC should be ~1200 times more effective at scattering
520 electrons. No energetic electron enhancements were observed during daytime periods,
521 consistent with the increased ionospheric absorption. We have also confirmed the persistent
522 occurrence of the wisp features east of the transmitter NWC. The enhancements can be
523 observed within a few degrees west of NWC, and are present in 95% of the nighttime orbital
524 data east of the transmitter for time periods when the transmitter is broadcasting. No
525 enhancements are observed when NWC is not broadcasting. This provides conclusive evidence
526 of the linkage between drift-loss cone electron flux enhancements and transmissions from
527 NWC. When contrasted with periods when NWC is non-operational, there are typically ~430
528 times more 100-260 keV resonant electrons present in the drift-loss cone across $L=1.67-1.9$ due
529 to NWC transmissions. Wisp events can have a fairly varied upper energy, ranging from 120-
530 410 keV, and also a wide range of enhancement factors, with the peak flux enhancement
531 ranging from ~1.2 to 2200 times. The variation in the resonance energies with geomagnetic
532 latitude has good agreement with that expected from first order equatorial cyclotron resonance
533 with NWC signals that have propagated through the plasmasphere inside ducts.

534 There are almost no wisp-like enhancements produced by the transmitter NPM, despite its
535 low-latitude location and relatively high output power. The lack of any wisp enhancement for
536 $L < 1.6$ suggests that non-ducted propagation is an inefficient mechanism for scattering
537 electrons, which explains the lower cutoff in L of the NWC-generated wisps and the lack of
538 NPM-generated wisps. The single example of an NPM-associated wisp is consistent with

539 transmissions from NPM coupling into a duct at $L=1.7$, with no significant scattering from the
540 non-ducted component known to be propagating through $L=1.2$ to 1.5.

541 Finally, we consider the likelihood that ducts are both sufficiently large in L and frequently-
542 occurring enough that a $\sim 95\%$ occurrence rate from $L=1.7-1.9$ could be explained solely due to
543 ducting. Previous studies of whistler-mode signals from the transmitter NAA, received in
544 Rothera station, Antarctica, show that ducting occurs across the L range in which we observe
545 NWC-driven enhancements, with an occurrence rate that is consistent with the 95% NWC wisp
546 occurrence rate reported in this paper.

547

548 **Acknowledgments.** CJR and MAC would like to acknowledge the funding support of the
549 LAPBIAT program (Contract RITA-CT-2006-025969) for supporting their time at the
550 Sodankylä Geophysical Observatory where they worked on this manuscript. The work of JAS,
551 MP, and JJB was supported by the Centre National d'Etudes Spatiales (CNES), while CJR is a
552 Guest Investigator inside the DEMETER program. We are grateful to the NSSDC at GSFC for
553 providing reports on radiation belt models, and the NOAA National Geophysical Data Center for
554 the POES data.

555 **References**

556 Abel, B., and Thorne, R. M.: Electron scattering loss in earth's inner magnetosphere-1. Dominant
557 physical processes, *J. Geophys. Res.*, 103, 2385-2396, 1998.

558 Abel, B., and Thorne, R. M.: Correction to "Electron scattering loss in earth's inner
559 magnetosphere, 1. Dominant physical processes" and " Electron scattering loss in earth's inner
560 magnetosphere, 2. Sensitivity to model parameters" by Abel, B. and Thorne, R.M., *J.*
561 *Geophys. Res.*, 104, 4627-4628, 1999.

562 Baker, D. N., Kanekal, S. G., Li, X., Monk, S. P., Goldstein, J., and Burch, J. L.: An extreme
563 distortion of the Van Allen belt arising from the 'Halloween' solar storm in 2003, *Nature*,
564 432(7019), pp. 878-880, 2004.

565 Berthelier, J.J., Godefroy, M., Leblanc, F., Malingre, M., Menvielle, M., Lagoutte, D., Brochot,
566 J.Y., Colin, F., Elie, F., Legendre, C., Zamora, P., Benoist, D., Chapuis, Y., Artru, J. (2006),
567 ICE, The electric field experiment on DEMETER, *Planet. Space Sci.*, 54 (5), Pages 456-471.

568 Carpenter, D.L., and R. R. Anderson (1992), An ISEE/whistler model of equatorial electron
569 density in the magnetosphere, *J. Geophys. Res.*, 97(2), 1097-1108.

570 Chang, H. C., and U. S. Inan (1983), Quasi-relativistic electron precipitation due to interactions
571 with coherent VLF waves in the magnetosphere, *J. Geophys. Res.*, 88, 318-328.

572 Clilverd, M. A., A. J. Smith, and N. R. Thomson (1991), The annual variation in quiet time
573 plasmaspheric electron-density, determined from whistler mode group delays, *Planet. Space*
574 *Sci.*, 39, 1059-1067.

575 Clilverd, M. A., N. R. Thomson, and A. J. Smith (1993), The influence of ionospheric absorption
576 on midlatitude whistler-mode signal occurrence from VLF transmitters, *J. Atmos. Terr. Phys.*,
577 55, 1469-1477.

578 Clilverd, M., and R. Horne (1996), Ground-based evidence of latitude-dependent cyclotron
579 absorption of whistler mode signals originating from VLF transmitters, *J. Geophys. Res.*,
580 101(A2), 2355-2367.

581 Clilverd, M., B. Jenkins, and N. Thomson (2000), Plasmaspheric storm time erosion, *J. Geophys.*
582 *Res.*, 105(A6), 12997-13008.

583 Clilverd, M. A., C. J. Rodger, R. J. Gamble, N. P. Meredith, M. Parrot, J.-J. Berthelier, and N. R.
584 Thomson (2008), Ground based transmitter signals observed from satellite: ducted or
585 nonducted?, *J. Geophys. Res.*, 113, A04211, doi:10.1029/2007JA012602, 2008.

586 Datlowe, D. (2006), Differences between transmitter precipitation peaks and storm injection
587 peaks in low-altitude energetic electron spectra, *J. Geophys. Res.*, 111, A12202,
588 doi:10.1029/2006JA011957.

589 Datlowe, D. W., and W. L. Imhof (1990), Cyclotron resonance precipitation of energetic
590 electrons from the inner magnetosphere, *J. Geophys. Res.*, 95, 6477-6491

591 Dupont, D. G.: Nuclear explosions in orbit., *Scientific American*, 68-75, June 2004.

592 Ferguson, J. A., and F. P. Snyder (1990), Computer programs for assessment of long wavelength
593 radio communications, Tech. Doc. 1773, Natl. Ocean Syst. Cent., San Diego, California.

594 Hess, W. N.: The radiation belt and magnetosphere, Blaisdell Pub. London, 1968.

595 Helliwell, R. A., *Whistlers and related ionospheric phenomena*, Stanford University Press,
596 Stanford, California, 1965.

597 Inan U. S., Bell, T. F., Bortnik, J., and Albert, J. M.: Controlled precipitation of radiation belt
598 electrons, *J. Geophys. Res.*, 108, 1186, doi:10.1029/2002JA009580, 2003.

599 Inan, U. S., M. Golkowski, M. K. Casey, R. C. Moore, W. Peter, P. Kulkarni, P. Kossey, E.
600 Kennedy, S. Meth, and P. Smit (2007), Subionospheric VLF observations of transmitter-
601 induced precipitation of inner radiation belt electrons, *Geophys. Res. Lett.*, 34, L02106,
602 doi:10.1029/2006GL028494.

603 Kulkarni, P., U. S. Inan, T. F. Bell, and J. Bortnik (2008), Precipitation Signatures of Ground-
604 Based VLF Transmitters, *J. Geophys. Res.*, doi:10.1029/2007JA012569, in press.

605 Li, X. L., and Temerin, M. A.: The electron radiation belt, *Space Sci. Rev.*, 95(1-2), 569-580,
606 2001.

607 Mahajan, K. K., and L. H. Brace (1969), Latitudinal observations of the thermal balance in the
608 nighttime protonosphere. *J. Geophys. Res.*, 74(21), 5099-5112.

609 Parrot, M., J. A. Sauvaud, J. J. Berthelier, and J. P. Lebreton (2007), First in-situ observations of
610 strong ionospheric perturbations generated by a powerful VLF ground-based transmitter,
611 *Geophys. Res. Lett.*, 34, L11111, doi:10.1029/2007GL029368.

612 Reeves, G. D., McAdams, K. L. Friedel, R. H. W., and O'Brien, T. P.: Acceleration and loss of
613 relativistic electrons during geomagnetic storms, *Geophys. Res. Lett.*, 30(10), 1529,
614 doi:10.1029/2002GL016513, 2003.

615 Rodger, C. J., Clilverd, M. A., and McCormick, R. J.: Significance of lightning generated
616 whistlers to inner radiation belt electron lifetimes, *J. Geophys. Res.*, 108(12), 1462,
617 10.1029/2003JA009906, 2003.

618 Rodger, C. J., M. A. Clilverd, Th. Ulich, P. T. Verronen, E. Turunen, and N. R. Thomson (2006),
619 The atmospheric implications of Radiation Belt Remediation, *Annales Geophys.*, 24(7), 2025 -
620 2041, SRef-ID: 1432-0576/ag/2006-24-2025.0020

621 Rodger, C. J., M. A. Clilverd, N. R. Thomson, R. J. Gamble, A. Seppälä, E. Turunen, N. P.
622 Meredith, M. Parrot, J. A. Sauvaud, and J.-J. Berthelier (2007a), Radiation belt electron
623 precipitation into the atmosphere: recovery from a geomagnetic storm, *J. Geophys. Res.*, 112,
624 A11307, doi:10.1029/2007JA012383.

625 Rodger, C. J., C. F. Enell, E. Turunen, M. A. Clilverd, N. R. Thomson, and P. T. Verronen,
626 Lightning-driven inner radiation belt energy deposition into the atmosphere: Implications for
627 ionisation-levels and neutral chemistry, *Annales Geophys.*, 25, 1745-1757, 2007b.

628 Sauvaud, J.A. T. Moreau, R. Maggiolo, J.-P. Treilhou, C. Jacquy, A. Cros, J. Coutelier, J.
629 Rouzaud, E. Penou and M. Gangloff (2006), High-energy electron detection onboard
630 DEMETER: The IDP spectrometer, description and first results on the inner belt, *Planet.*
631 *Space. Sci.*, 54 (5), 502-511.

632 Sauvaud, J. A., R. Maggilo, C. Jacquy, M. Parrot, J.-J. Berthelier, R. J. Gamble, and C. J.
633 Rodger, Radiation belt electron precipitation due to VLF transmitters: satellite observations,
634 Geophys. Res. Lett., (in press), 2008.

635 Steer, I.: Briefing: High-altitude nuclear explosions; Blind, deaf and dumb, Janes Defense
636 Weekly, 20-23, 23 October 2002.

637 Teague, M. and J. Vette, *The inner zone electron model AE-5*, National Space Science Data
638 Center, Rep. NSSDC 72-10, Greenbelt, Md., 1972.

639 Thomson, N. R. (1987), Experimental observations of very low latitude man-made whistler-
640 mode signals, J. Atmos. Terr. Phys., 49, 309-319.

641 Thomson, N. R. (1989), Reradiation of VLF radio-waves from mountain ranges, J. Atmos. Terr.
642 Phys., 51, 339-349.

643 U.S. Congress, Report of the commission to assess United States national security, space
644 management and organization, Public Law 106-65, Chapter II: Space: Today and the Future,
645 21-22, 11 January 2001. (available from <http://www.space.gov/docs/fullreport.pdf>)

646 Van Allen, J. A.: Energetic particles in the Earth's external magnetic field, in *Discovery of the*
647 *Magnetosphere*, edited by C. S. Gillmor and J. R. Spreiter, History of Geophysics, 7, 235-251,
648 American Geophysical Union, Washington, D.C., 1997.

649 Van Allen, J. A., Ludwig, G. H., Ray, E. C., and McIlwain, C. E.: Observation of high intensity
650 radiation by satellites 1958 Alpha and Gamma, *Jet Propulsion*, 28, 588-592, 1958.

651 Winter, J., et al, A proposed large deployable space structures experiment for high power, large
652 aperture missions in MEO, 2004 IEEE Aerospace Conference Proceedings, Volume 1,
653 10.1109/AERO.2004.1367636, 6-13 March 2004.

654 _____

655 Jean-Jacques Berthelier, Centre d'Etudes des Environnements Terrestre et Planétaires, 4
656 Avenue de Neptune, Saint Maur des Fosses, France. (email: jean-
657 jacques.berthelier@cetp.ipsl.fr).

658 M. A. Clilverd, Physical Sciences Division, British Antarctic Survey, High Cross, Madingley
659 Road, Cambridge CB3 0ET, England, U.K. (e-mail: M.Clilverd@bas.ac.uk).

660 R. J. Gamble, R. J. McCormick, C. J. Rodger, S. L. Stewart, and N. R. Thomson, Department
661 of Physics, University of Otago, P.O. Box 56, Dunedin, New Zealand. (email:
662 rgamble@physics.otago.ac.nz, rmccormick@physics.otago.ac.nz, crodger@physics.otago.ac.nz,
663 sstewart@physics.otago.ac.nz, thomson@physics.otago.ac.nz).

664 M. Parrot, Laboratoire de Physique et Chimie de l'Environnement, 3A Avenue de la Recherche
665 Scientifique, 45071 Orleans Cedex 2, France (email: mparrot@cnrs-orleans.fr).

666 J. A. Sauvaud, Centre d'Etude Spatiale des Rayonnements, 9 Avenue du Colonel Roche 31028,
667 Toulouse Cedex 4, France (email: sauvaud@cesr.fr)

668

669

670 GAMBLE ET AL.: VLF TX DRIVEN ELECTRON PRECIPITATION

671

672 **Figure Captions**

673 **Figure 1.** Average power received by the ICE instrument on DEMETER at 19.8 kHz for night
674 (left) and day (right) orbits. The locations shown are those found by tracing from the satellite
675 down the field line to 100 km altitude. The subionospheric path from NWC to Dunedin is
676 shown, as are L-shell contours. The dark diamond in the northern hemisphere indicates the
677 conjugate location of the transmitter. [See the online version for the color version of this
678 figure].

679 **Figure 2.** Typical UT variation in transmissions from the VLF station NWC, received at
680 Dunedin, New Zealand 21-27 August 2005. Nighttimes correspond to the periods with higher
681 amplitudes. This plot presents 1-minute average amplitudes demonstrating the near-constant
682 operation of this transmitter.

683 **Figure 3.** Examples of typical drift-loss cone electron flux enhancements, termed wisps, seen
684 from $L=1.6-1.8$ in the IDP observations during a DEMETER orbit. This shows four examples
685 of the absolute flux measurements in units of electrons $\text{cm}^{-2}\text{s}^{-1}\text{sr}^{-1}\text{keV}^{-1}$ during wisp events.
686 [See the online version for the color version of this figure].

687 **Figure 4.** Dunedin-received 1-minute average NWC amplitudes in June 2005 during a period
688 in which NWC ceased transmitting for ~ 14 days. The circles indicate the times DEMETER
689 nighttime orbits within 25° eastwards of NWC, while the crosses show orbits in which wisps
690 were observed.

691 **Figure 5.** The effect of the NWC transmissions seen in the >100 keV electron observations
692 from the POES spacecraft. The upper panel shows the sum of all the >100 keV electron counts
693 from the MEPED 90 degree detector for the period 1 August -31 December 2007 when NWC

694 was not operating. The lower panel shows the ratio between the period 1 Jan-31 May 2007 and
 695 the upper panel. NWC was operating normally in the first half of 2007. [See the online version
 696 for the color version of this figure].

697 **Figure 6.** Examples of the relative electron flux enhancements for the four wisp events shown
 698 in Figure 3. The wisp enhancements are show relative to a reference background spectrum
 699 when NWC was not transmitting and no wisp enhancement was present. [See the online
 700 version for the color version of this figure].

701 **Figure 7.** Variation with L of the first-order cyclotron resonant energy with waves of 19.8 kHz
 702 (black), and the plasmaspheric electron number density used in this calculation (dashed gray).
 703 The crosses mark the mean L and energy for typical wisps as described in Table 2.

704 **Figure 8.** Examples of DEMETER IDP observations east of the VLF transmitter NPM at
 705 night. The left panel shows the typical situation where no wisp is present. The right panel
 706 shows a rare observation of a wisp likely generated by ducted transmissions from NPM. [See
 707 the online version for the color version of this figure].

708 **Figure 9.** Amplitude of received NAA whistler-mode signals arriving at Rothera (Antarctica)
 709 as a function of group delay time. The group delays which are typical of night time ducted
 710 propagation have L -values in the range $L=1.6-2.6$ (as shown by two horizontal dashed lines).
 711 Also shown on the plot are subionospheric mountain reflections, which have very little delay
 712 compared with the arrival time of the direct, subionospheric signal.

713

	Day	Night
East	(43) 0	(39) 36
West	(46) 0	(45) 10

714

715 **Table 1.** Summary of wisp observations (1) 25° longitude west of NWC and (2) and 25°
 716 longitude east of NWC, observed during nighttime or daytime orbits. The first value given is
 717 the number of half-orbits examined, the second gives the number of those half-orbits containing
 718 wisps.

719

720

721

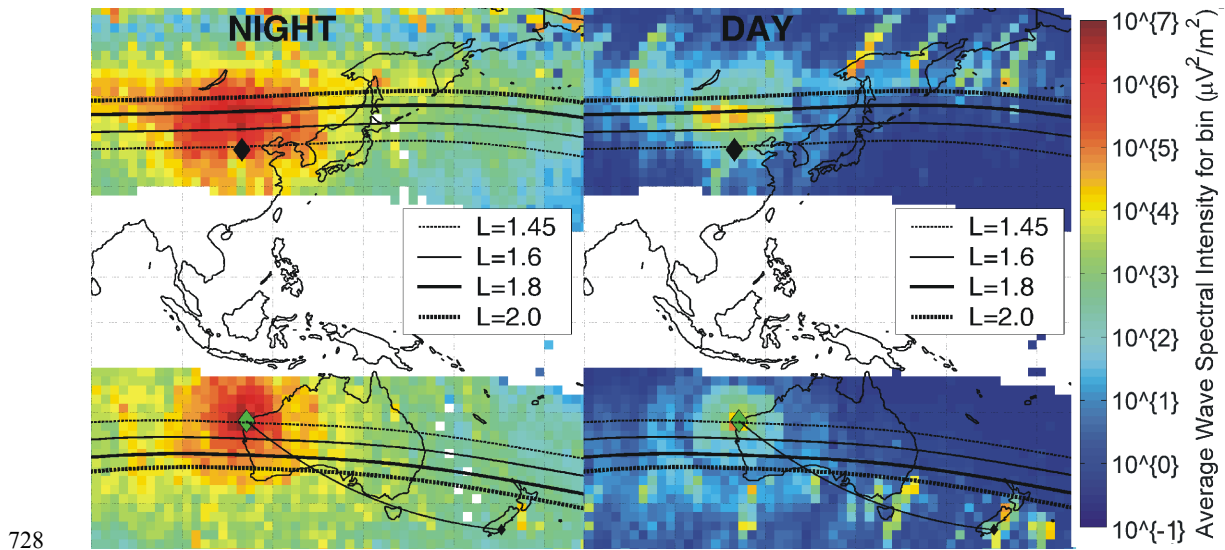
	Lower L	Mid L	Upper L	Lower E (keV)	Mid E (keV)	Upper E (keV)	Flux Enhancement
Mean	1.67	1.77	1.90	103	168	262	429
Median	1.67	1.78	1.91	93	159	257	175

722

723 **Table 2.** Summary of typical wisp properties for the 46 events observed in August-September
 724 2005. The Peak Flux Enhancement is the relative increase factor in the quasi-trapped electron
 725 fluxes.

726

727



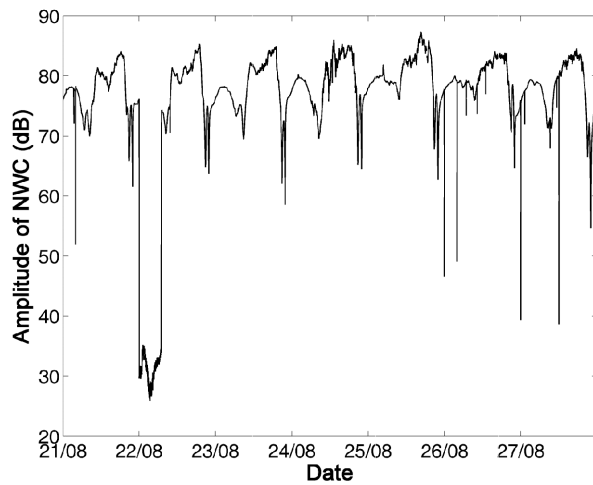
728

729 **Figure 1.** Average power received by the ICE instrument on DEMETER at 19.8 kHz for night
 730 (left) and day (right) orbits. The locations shown are those found by tracing from the satellite
 731 down the field line to 100 km altitude. The subionospheric path from NWC to Dunedin is
 732 shown, as are L-shell contours. The dark diamond in the northern hemisphere indicates the
 733 conjugate location of the transmitter. [See the online version for the color version of this
 734 figure].

735

736

737

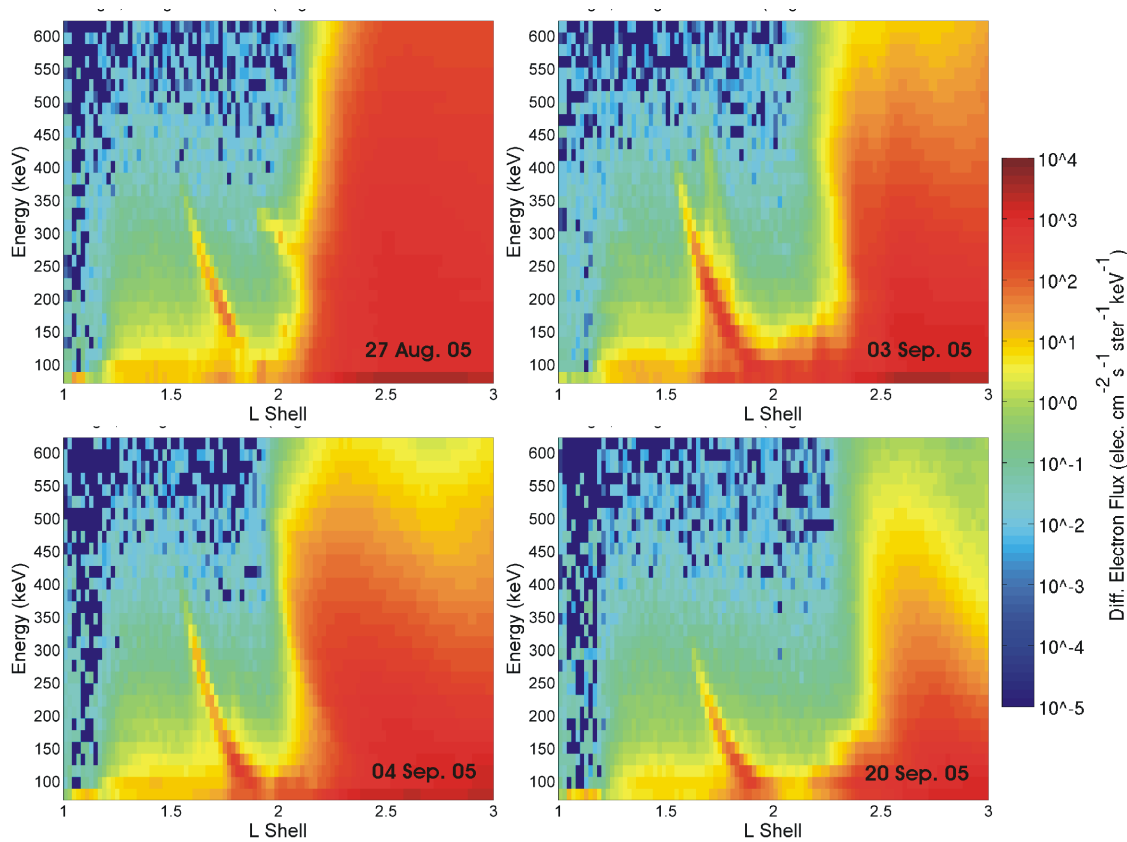


738

739 **Figure 2.** Typical UT variation in transmissions from the VLF station NWC, received at
740 Dunedin, New Zealand 21-27 August 2005. Nighttimes correspond to the periods with higher
741 amplitudes. This plot presents 1-minute average amplitudes demonstrating the near-constant
742 operation of this transmitter.

743

744

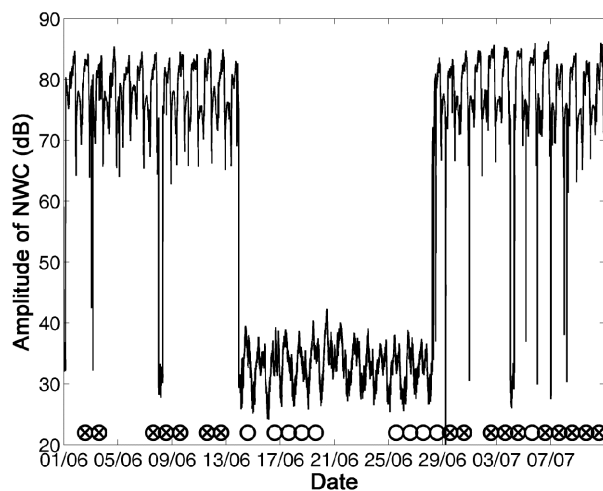


745

746 **Figure 3.** Examples of typical drift-loss cone electron flux enhancements, termed wisps, seen
 747 from $L=1.6-1.8$ in the IDP observations during a DEMETER orbit. This shows four examples
 748 of the absolute flux measurements in units of electrons $\text{cm}^{-2}\text{s}^{-1}\text{str}^{-1}\text{keV}^{-1}$ during wisp events.

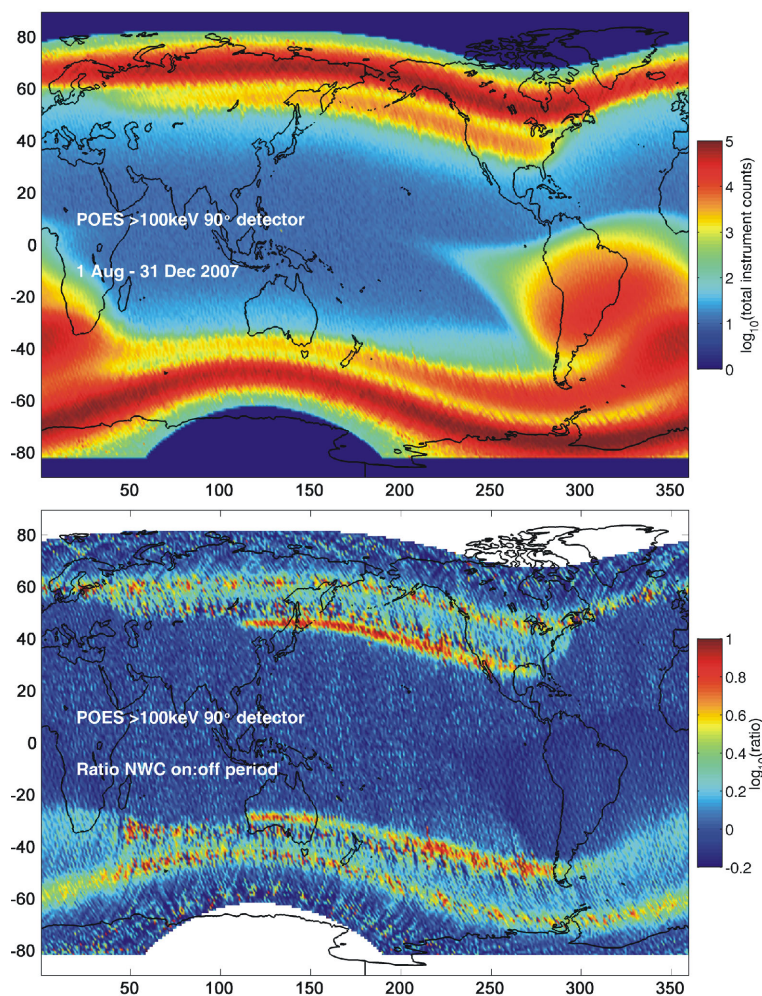
749 [See the online version for the color version of this figure].

750



751

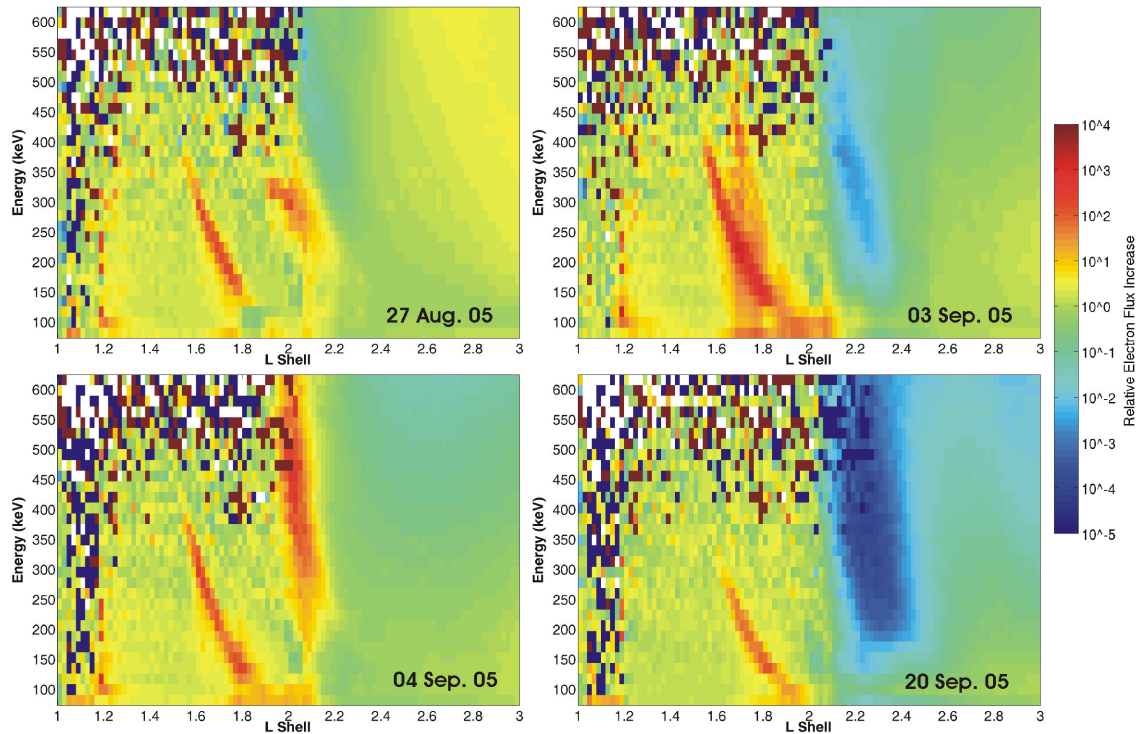
752 **Figure 4.** Dunedin-received 1-minute average NWC amplitudes in June 2005 during a period
753 in which NWC ceased transmitting for ~14 days. The circles indicate the times DEMETER
754 nighttime orbits within 25° eastwards of NWC, while the crosses show orbits in which wisps
755 were observed.
756



757
758 **Figure 5.** The effect of the NWC transmissions seen in the >100 keV electron observations
759 from the POES spacecraft. The upper panel shows the sum of all the >100 keV electron counts
760 from the MEPED 90 degree detector for the period 1 August -31 December 2007 when NWC
761 was not operating. The lower panel shows the ratio between the period 1 Jan-31 May 2007 and

762 the upper panel. NWC was operating normally in the first half of 2007. [See the online version
763 for the color version of this figure].

764

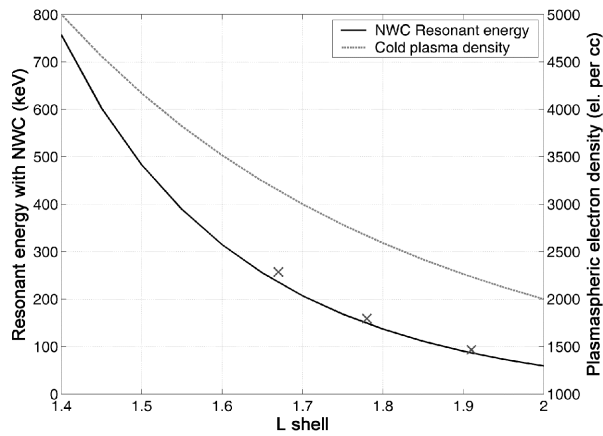


765

766 **Figure 6.** Examples of the relative electron flux enhancements for the four wisp events shown
767 in Figure 3. The wisp enhancements are show relative to a reference background spectrum
768 when NWC was not transmitting and no wisp enhancement was present. [See the online
769 version for the color version of this figure].

770

771



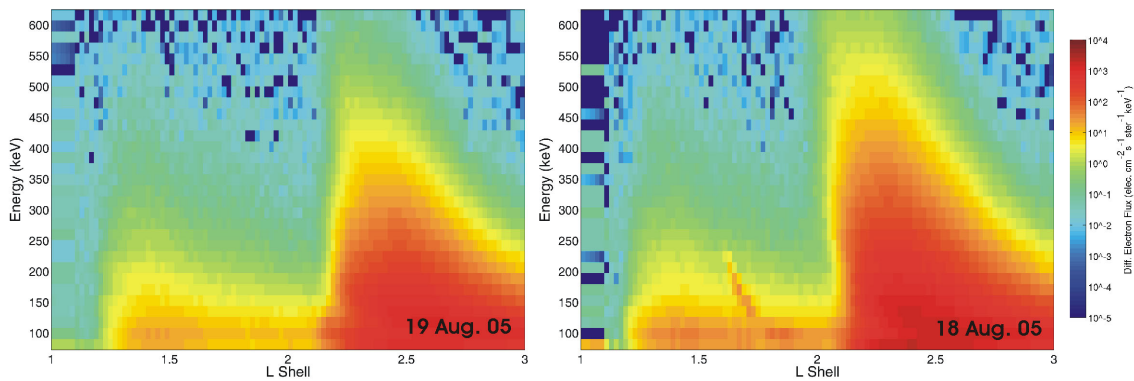
772

773 **Figure 7.** Variation with L of the first-order cyclotron resonant energy with waves of 19.8 kHz
 774 (black), and the plasmaspheric electron number density used in this calculation (dashed gray).

775 The crosses mark the median L and energy for typical wisps as described in Table 2.

776

777

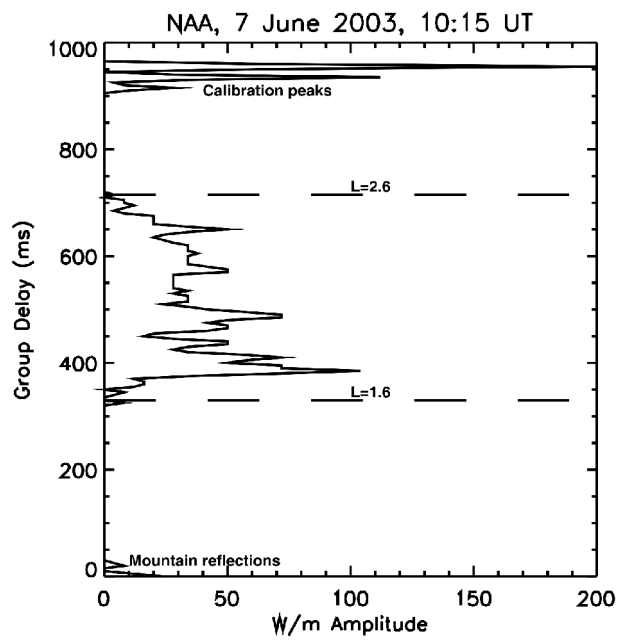


778

779 **Figure 8.** Examples of DEMETER IDP observations east of the VLF transmitter NPM at
 780 night. The left panel shows the typical situation where no wisp is present. The right panel
 781 shows a rare observation of a wisp likely generated by ducted transmissions from NPM. [See
 782 the online version for the color version of this figure].

783

784



785

786 **Figure 9.** Amplitude of received NAA whistler-mode signals arriving at Rothera (Antarctica)
 787 as a function of group delay time. The group delays which are typical of night time ducted
 788 propagation have L -values in the range $L=1.6-2.6$ (as shown by two horizontal dashed lines).
 789 Also shown on the plot are subionospheric mountain reflections, which have very little delay
 790 compared with the arrival time of the direct, subionospheric signal.

791